Definition of Two Angiogenic Pathways by Distinct α_v Integrins

Martin Friedlander, Peter C. Brooks, Robert W. Shaffer, Christine M. Kincaid, Judith A. Varner, David A. Cheresh

Angiogenesis depends on cytokines and vascular cell adhesion events. Two cytokine-dependent pathways of angiogenesis were shown to exist and were defined by their dependency on distinct vascular cell integrins. In vivo angiogenesis in corneal or chorioallantoic membrane models induced by basic fibroblast growth factor or by tumor necrosis factor–α depended on $\alpha_v\beta_3$, whereas angiogenesis initiated by vascular endothelial growth factor, transforming growth factor–α, or phorbol ester depended on $\alpha_v\beta_5$. Antibody to each integrin selectively blocked one of these pathways, and a cyclic peptide antagonist of both integrins blocked angiogenesis stimulated by each cytokine tested. These pathways are further distinguished by their sensitivity to calphostin C, an inhibitor of protein kinase C that blocked angiogenesis potentiated by $\alpha_v\beta_5$ but not by $\alpha_v\beta_3$.

Angiogenesis, the growth of new blood vessels, occurs in most tissues and can be induced by a variety of cytokines (*1*). However, vascular cells proliferate in an anchorage-dependent manner, which suggests that adhesion-mediated signals may be important in the growth of new blood vessels (*2*). The dependence of angiogenesis on vascular cell adhesive events in vivo (*3*, *4*) is evidenced by the fact that antagonists of $\alpha_v\beta_3$ integrin block angiogenesis on chick chorioallantoic membrane (CAM) induced by basic fibroblast growth factor (bFGF) and fragments of human tumors. In this model, $\alpha_v\beta_3$ promoted a survival signal that facilitated blood vessel growth and differentiation (*4*). In addition, this integrin also potentiated blood vessel maturation in developing quail (*5*). Therefore, it is likely that signaling events potentiated by both cytokines and adhesion receptors are critical to the growth of new blood vessels.

Although vascular cells respond to multiple cytokines, they also express a variety of integrin adhesion receptors (*6*–*9*). In fact, a number of the vascular cell integrins are functionally and structurally homologous, suggesting some level of biologic redundancy. Therefore, we compared the roles of the functionally homologous integrins $\alpha_v\beta_3$ and $\alpha_v\beta_5$ in ocular angiogenesis stimulated by the distinct cytokines bFGF and vascular endothelial cell growth factor (VEGF). These cytokines are associated with ocular neovascularization (*10*–*12*). To examine the role of these integrins in ocular angiogenesis, we implanted pellets containing either bFGF or VEGF into rabbit corneas. A series of eight animals was used for paired eye experiments, and each animal received a Hydron [poly(hydroxyethyl) methacrylate; Interferon Sciences, New Brunswick, New Jersey] implant containing cytokine and monoclonal antibody (mAb) LM609 (anti-$\alpha_v\beta_3$) in one cornea, and cytokine and mAb P1F6 (anti-$\alpha_v\beta_5$) or nonimmune immunoglobulin in the other cornea (Fig. 1) (*13*). The mAb LM609 inhibited bFGF-induced angiogenesis by 86% ($P < 0.005$, Student's t test) compared with eyes treated with mAb P1F6, and by 72% compared with immunoglobulin G controls ($P < 0.005$). However, when VEGF was used to induce angiogenesis, P1F6 reduced angiogenesis by 60% compared with LM609 ($P < 0.03$; Fig. 1). Preexisting perilimbal vessels were unaffected by either antibody, suggesting that the effects observed were restricted to newly forming blood vessels in the cornea. That $\alpha_v\beta_5$ functions in VEGF-induced angiogenesis may be clinically relevant, because VEGF is reported to be temporally and spatially associated with ischemia-induced ocular angiogenesis (*11*) and is increased in intraocular fluids obtained from patients with active neovascular eye disease (*12*).

To confirm these results, we examined another model of angiogenesis, the chick CAM (Fig. 2, A and B). The mAb LM609 (anti-$\alpha_v\beta_3$) disrupted angiogenesis induced by bFGF, whereas mAb P1F6 (anti-$\alpha_v\beta_5$) had no effect. However, as shown in the preceding corneal model, LM609 had only a slight effect on angiogenesis on the CAM stimulated by VEGF (Fig. 2, A and B), whereas P1F6 blocked this event. As predicted, a cyclic peptide antagonist (RGDfV) specific for both $\alpha_v\beta_3$ and $\alpha_v\beta_5$ (*14*) abolished angiogenesis induced by either cytokine (Fig. 2, C and D). These results, together with those from the cornea, suggest that bFGF- and VEGF-induced angiogenesis depend on distinct α_v integrins.

To extend these findings, we examined

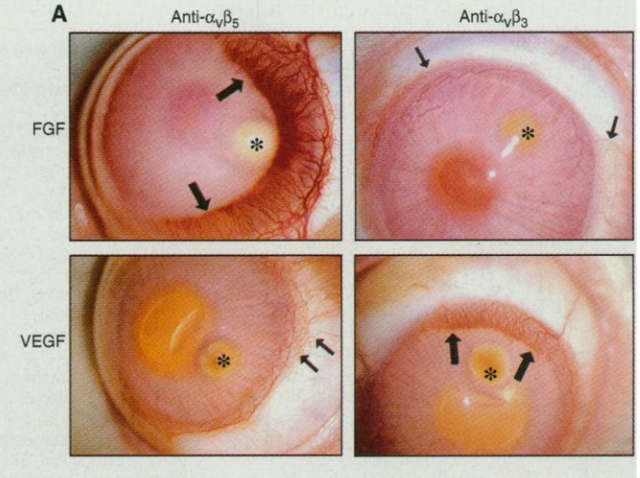

Fig. 1. Inhibition of cytokine-induced rabbit corneal angiogenesis by antibody antagonists of α_v integrins. (**A**) Hydron pellets (asterisks) containing Carafate-stabilized cytokine (750 μg; bFGF, top, or VEGF, bottom) and mAb to α_v integrin antibody (40 μg; P1F6 mAb to $\alpha_v\beta_5$, left, or LM609 mAb to $\alpha_v\beta_3$, right) were surgically implanted into paired rabbit corneas (left eye, left; right eye, right) and observed daily for 12 days. Photographs were taken on day 10 after implantation, the time at which neovascularization is maximal. Corneal angiogenesis (large arrows) with edema is prominent in upper left and lower right panels, whereas normal conjunctival limbal vessels (small arrows) appear in upper right and lower left panels. Magnification, ×2.2. (**B**) Angiogenesis was stimulated by either bFGF (left panel) or VEGF (right panel). Histograms show mean neovascular area ± SE ($n = 8$ for each of two series) after treatment with P1F6 or LM609. LM609 reduced angiogenesis by 86% ($P < 0.005$, Student's t test) when compared with treatment of the paired cornea (same animal) with P1F6. When VEGF was used to stimulate angiogenesis, the opposite effect was observed; P1F6 reduced the mean area of neovascularization by 60% ($P < 0.03$, paired t test) compared with LM609-treated paired eyes. Cytokine- and antibody-containing Hydron pellets were prepared and surgically implanted as described (*13*).

M. Friedlander, R. W. Shaffer, C. M. Kincaid, Robert Mealey Laboratory for the Study of Macular Degenerations, Department of Cell Biology, Scripps Research Institute, La Jolla, CA 92037, USA.
P. C. Brooks and D. A. Cheresh, Departments of Immunology and Vascular Biology, Scripps Research Institute, La Jolla, CA 92037, USA.
J. A. Varner, Department of Medicine, University of California, San Diego, La Jolla, CA 92093, USA.

angiogenesis on the chick CAM induced with a series of cytokines in the presence of anti-$\alpha_v\beta_3$ or anti-$\alpha_v\beta_5$. Angiogenesis was induced with bFGF, VEGF, tumor necrosis factor–α (TNF-α), transforming growth factor–α (TGF-α), or phorbol 12-myristate 13-acetate (PMA). One day later, embryos were injected with a single dose of mAb LM609 or mAb P1F6 (Fig. 3). LM609 blocked angiogenesis in response to bFGF and TNF-α, yet had minimal effect on angiogenesis induced by VEGF, TGF-α, or PMA. In contrast, P1F6 blocked angiogenesis induced by VEGF, TGF-α, and PMA, but had minimal effects on that induced by bFGF or TNF-α.

The phorbol ester PMA, a potent inducer of angiogenesis, is capable of activating protein kinase C (PKC), an intracellular family of serine-threonine kinases. Therefore, we also examined the effects of calphostin C, a PKC inhibitor, on angiogenesis on the chick CAM (Fig. 3). Calphostin C blocked angiogenesis induced by PMA, VEGF, and TGF-α, but had only a small effect on bFGF- or TNF-α–mediated angiogenesis. These results suggest the presence of two pathways of angiogenesis: one that depends on $\alpha_v\beta_3$ and that is largely independent of PKC, and a second that is potentiated by $\alpha_v\beta_5$ but also critically depends on PKC activation. These data are consistent with our previous observations that cell motility mediated by $\alpha_v\beta_5$, but not by $\alpha_v\beta_3$, depends on prior activation of a PKC-dependent signaling pathway (*15*).

Angiogenesis is associated with an array of pathologic processes, including cancer, blindness, and inflammatory disease (*1*, *3*). Our results suggest that antagonists of $\alpha_v\beta_3$ and $\alpha_v\beta_5$ may be effective in treating such processes. The LM609 mAb to $\alpha_v\beta_3$ causes variable regression of four types of human tumors grown on chick CAM (*4*). It is conceivable that tumors showing less susceptibility to LM609 might secrete several cytokines, including one such as VEGF that promotes angiogenesis in an $\alpha_v\beta_5$-dependent manner. This contention is supported by the finding that the cyclic peptide RGDfV (Fig.

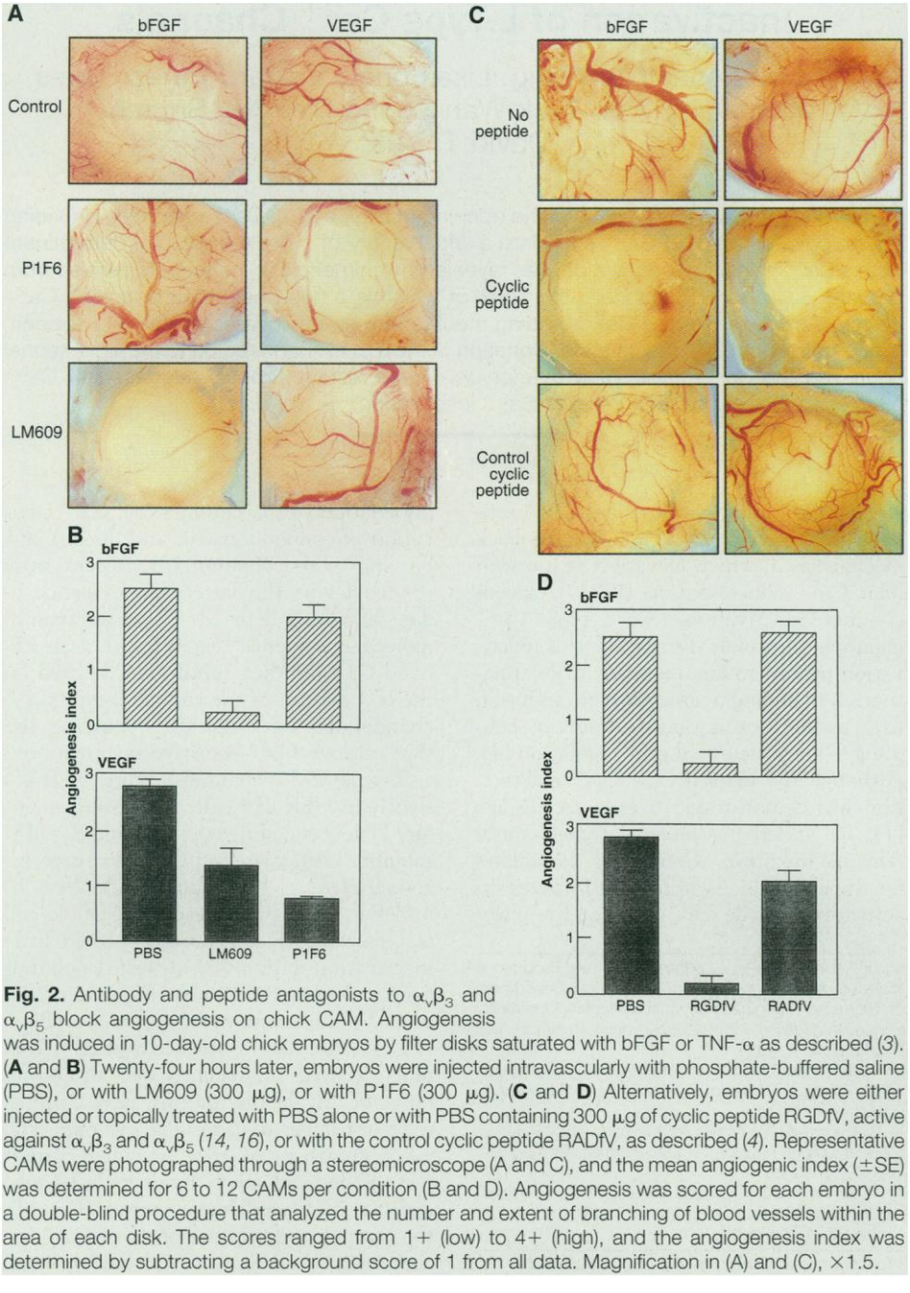

Fig. 2. Antibody and peptide antagonists to $\alpha_v\beta_3$ and $\alpha_v\beta_5$ block angiogenesis on chick CAM. Angiogenesis was induced in 10-day-old chick embryos by filter disks saturated with bFGF or TNF-α as described (*3*). (**A** and **B**) Twenty-four hours later, embryos were injected intravascularly with phosphate-buffered saline (PBS), or with LM609 (300 μg), or with P1F6 (300 μg). (**C** and **D**) Alternatively, embryos were either injected or topically treated with PBS alone or with PBS containing 300 μg of cyclic peptide RGDfV, active against $\alpha_v\beta_3$ and $\alpha_v\beta_5$ (*14*, *16*), or with the control cyclic peptide RADfV, as described (*4*). Representative CAMs were photographed through a stereomicroscope (A and C), and the mean angiogenic index (±SE) was determined for 6 to 12 CAMs per condition (B and D). Angiogenesis was scored for each embryo in a double-blind procedure that analyzed the number and extent of branching of blood vessels within the area of each disk. The scores ranged from 1+ (low) to 4+ (high), and the angiogenesis index was determined by subtracting a background score of 1 from all data. Magnification in (A) and (C), ×1.5.

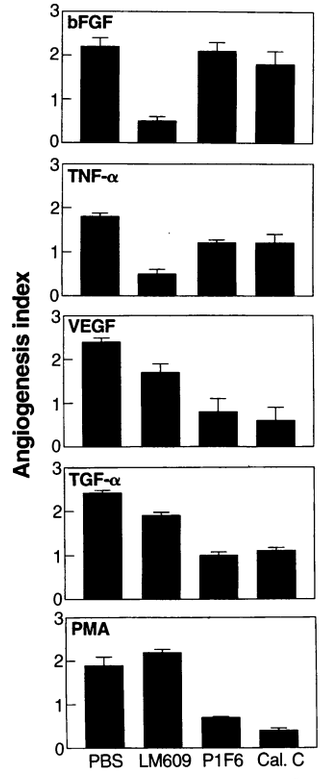

Fig. 3. Effect of anti-$\alpha_v\beta_3$, anti-$\alpha_v\beta_5$, and calphostin C (Cal. C) on CAM angiogenesis induced by multiple cytokines. CAM tissue from 10-day-old chick embryos was stimulated by filter disks saturated with 1.0 μg/ml of bFGF, TNF-α, VEGF, or TGF-α, or with 20 ng/ml of PMA. Embryos were then injected intravascularly with 300 μg per 0.1 ml per embryo of mAbs LM609 (anti-$\alpha_v\beta_3$) or P1F6 (anti-$\alpha_v\beta_5$) or topically treated with 100 nM calphostin C (0.1 ml) daily for 3 days. On day 13, filter disks and associated CAM tissue were dissected and analyzed for angiogenesis with a stereomicroscope. Angiogenesis was scored in a double-blind procedure that analyzed the number and extent of branching of blood vessels within the area of each disk. The scores for angiogenesis ranged from 1+ (low) to 4+ (high). The angiogenesis index was determined by subtracting a background score of 1 from all data. Experiments were repeated two to four times with five to six embryos per condition.

2), which blocks both α_v integrins (*16*), showed the greatest antiangiogenic and antitumoral activity when compared with either anti-$\alpha_v\beta_3$ alone or anti-$\alpha_v\beta_5$ alone (*16*).

Most ocular diseases that cause catastrophic loss of vision have as a common pathologic feature the growth of new blood vessels. Although ischemia-associated retinal neovascular diseases such as proliferative diabetic retinopathy are associated with increased VEGF (*12*), nonischemic subretinal neovascular diseases such as age-related macular degeneration have no such clear association. Our observation that VEGF-stimulated angiogenesis proceeds by an integrin-mediated angiogenic pathway distinct from that stimulated by FGF supports the concept that different pathogenetic mechanisms may operate in retinal and subretinal diseases (*17*).

Angiogenesis is a critical biologic process and, as such, may depend on redundant molecular events that not only initiate blood vessel cell proliferation but also regulate the invasion and, ultimately, the differentiation of newly forming vessels. Redundancy in this process is supported by an experiment of nature, Glanzmann's thrombasthenia, in which individuals lacking expression of the β_3 integrin gene nevertheless develop fully mature blood vessels. Thus, an alternative angiogenic mechanism must exist in the absence of $\alpha_v\beta_3$. The evidence presented here suggests that $\alpha_v\beta_5$ can provide such a mechanism of biologic redundancy. We conclude that there are at least two cytokine-dependent pathways leading to angiogenesis in vivo, and these are distinguished by their dependency on specific α_v integrins and on the intracellular serine-threonine kinase PKC.

REFERENCES AND NOTES

1. J. Folkman and Y. Shing, *J. Biol. Chem.* **267**, 10931 (1992); P. A. D'Amore and R. W. Thompson, *Annu. Rev. Physiol.* **49**, 453 (1987); J. Folkman, *Nature Med.* **1**, 27 (1995); D. Ingber and J. Folkman, *Cell Biol.* **109**, 317 (1989); D. Weinstat-Saslow and P. Steeg, *FASEB J.* **8**, 401 (1994).
2. J. E. Meredith, B. Fazeli, M. A. Schwartz, *Mol. Biol. Cell.* **4**, 953 (1993).
3. P. C. Brooks, R. A. F. Clark, D. A. Cheresh, *Science* **264**, 569 (1994).
4. P. C. Brooks *et al.*, *Cell* **79**, 1157 (1994).
5. C. J. Drake, D. A. Cheresh, C. D. Little, *J. Cell Sci.* **108**, 2655 (1995).
6. D. A. Cheresh, *Proc. Natl. Acad. Sci. U.S.A.* **84**, 6471 (1987).
7. D. I. Leavesley, M. A. Schwartz, M. Rosenfeld, D. A. Cheresh, *J. Cell Biol.* **121**, 163 (1993).
8. J. Enenstein and R. H. Kramer, *J. Invest. Dermatol.* **103**, 381 (1994).
9. D. A. Cheresh, S. A. Berliner, V. Vicente, V. Z. Ruggeri, *Cell* **58**, 945 (1989).
10. P. A. D'Amore, *Invest. Ophthalmol. Vis. Sci.* **35**, 3974 (1994).
11. J. W. Miller *et al.*, *Am. J. Pathol.* **145**, 574 (1994).
12. L. P. Aiello *et al.*, *N. Engl. J. Med.* **331**, 1480 (1994).
13. R. J. D'Amato, M. S. Loughnan, E. Flynn, J. Folkman, *Proc. Natl. Acad. Sci. U.S.A.* **91**, 4082 (1994); R. Shaffer and M. Friedlander, in *NATO ASI on Molecular, Cellular, and Clinical Aspects of Angiogenesis*, M. E. Maragoudakis, Ed. (Plenum, New York, in press). We modified the Hydron pellets so that endotoxin-free antibody was incorporated directly into the pellet. Eyes were examined and photographed daily through a Wild operating microscope. Photographs were recorded on Kodak Ektachrome 64T slide film, and images were converted for computer-assisted quantitation with Molecular Analyst 1.1 software (Bio-Rad) after acquisition through a Model GS670 imaging densitometer.
14. M. Pfaff *et al.*, *J. Biol. Chem.* **269**, 20233 (1994).
15. R. L. Klemke, M. Yebra, E. M. Bayna, D. A. Cheresh, *J. Cell Biol.* **127**, 859 (1994).
16. P. C. Brooks and D. A. Cheresh, unpublished data.
17. M. Friedlander, paper presented at the Retina Society Meeting, Santa Fe, NM, 8 September 1995.

18. Supported by grants to M.F. from the Lions Sightfirst Diabetic Retinopathy Research Program of the American Diabetes Association, the Scripps Clinic Department of Academic Affairs Clinical Research Program, and the Ralwhbnbg Fund, and by grants to D.A.C. from the National Cancer Institute and the Heart, Lung, and Blood Institute at the National Institutes of Health. D.A.C. is a recipient of an American Cancer Society Faculty Research Award. We thank S. Fallon, M. Sugita, and M. Toth for helpful comments and suggestions. We also thank S. Goodman and A. Jonczyk (E. Merck, KGaA, Darmstadt) for providing peptides and supporting evidence that cyclic peptide RGDfV (EP 0578 083 A2) blocks both $\alpha_v\beta_3$ and $\alpha_v\beta_5$. Sucralfate (Carafate) was a gift of Marion–Merrell Dow Pharmaceuticals (Cincinnati, OH).

2 June 1995; accepted 26 September 1995

Essential Ca^{2+}-Binding Motif for Ca^{2+}-Sensitive Inactivation of L-Type Ca^{2+} Channels

Marita de Leon, Yan Wang, Lisa Jones, Edward Perez-Reyes, Xiangyang Wei, Tuck Wah Soong, Terry P. Snutch, David T. Yue*

Intracellular calcium (Ca^{2+}) inhibits the opening of L-type (α_{1C}) Ca^{2+} channels, providing physiological control of Ca^{2+} entry into a wide variety of cells. A structural determinant of this Ca^{2+}-sensitive inactivation was revealed by chimeric Ca^{2+} channels derived from parental α_{1C} and α_{1E} channels, the latter of which is a neuronal channel lacking Ca^{2+} inactivation. A consensus Ca^{2+}-binding motif (an EF hand), located on the α_{1C} subunit, was required for Ca^{2+} inactivation. Donation of the α_{1C} EF-hand region to the α_{1E} channel conferred the Ca^{2+}-inactivating phenotype. These results strongly suggest that Ca^{2+} binding to the α_{1C} subunit initiates Ca^{2+} inactivation.

L-type Ca^{2+} channels manifest Ca^{2+}-sensitive inactivation (*1*), a biological feedback mechanism in which elevation of intracellular Ca^{2+} concentration ($[Ca^{2+}]$) speeds channel inactivation. As L-type Ca^{2+} channels are widely distributed, this inactivation process influences many cellular activities, including neuroendocrine secretion (*2*), cardiac excitation-contraction coupling (*3*), and neuronal gene regulation (*4*). Although the existence of Ca^{2+} inactivation was demonstrated over a decade ago (*1*), its underlying molecular mechanism remains unknown. Competing candidates for the chemical "switch" that initiates inactivation include Ca^{2+}-induced (de)phosphorylation of the channel (*5*), Ca^{2+} activation of calmodulin (*6*), and direct Ca^{2+} binding to the channel (*7*). Recent work (*8–10*) favors the latter, but evidence to date has been debated. Here, we present molecular evidence suggesting that an EF-hand Ca^{2+}-binding motif (*11*), located on the α_{1C} subunit of the cardiac L-type Ca^{2+} channel, provides the Ca^{2+} binding site that initiates Ca^{2+}-sensitive inactivation.

L-type Ca^{2+} channels, expressed transiently in HEK 293 cells from complementary DNAs encoding α_{1C} (*12*) and β_{2a} (*13*) subunits (*14*), possessed Ca^{2+}-sensitive inactivation (Fig. 1, A through C). With 10 mM Ba^{2+} as the charge carrier, whole-cell α_{1C} currents (Fig. 1A, top) showed little inactivation during 300-ms test depolarizations, as expected from the high selectivity of Ca^{2+} inactivation for Ca^{2+} over Ba^{2+} (*1*). Average data confirmed that Ba^{2+} currents decayed only slightly over the entire range of test depolarizations; peak currents were just larger than residual currents (Fig. 1A, bottom). By contrast, specimen current records decayed much more with 10 mM external Ca^{2+} as charge carrier (Fig. 1B, top), which suggests the onset of Ca^{2+} inactivation. Averages of peak and residual

M. de Leon, Y. Wang, L. Jones, D. T. Yue, Program in Molecular and Cellular Systems Physiology, Department of Biomedical Engineering, Johns Hopkins University School of Medicine, 720 Rutland Avenue, Baltimore, MD 21205, USA.
E. Perez-Reyes, Department of Physiology, Loyola University Chicago, 2160 South First Avenue, Maywood, IL 60153, USA.
X. Wei, Institute for Molecular Medicine and Genetics, Medical College of Georgia, 1120 15th Street, Augusta, GA 30912, USA.
T. W. Soong and T. P. Snutch, Biotechnology Laboratory, University of British Columbia, Vancouver, British Columbia V6T 1Z3, Canada.
*To whom correspondence should be addressed.